

Deadly disasters in the Southeastern South America: Flash floods and landslides of February 2022 in Petrópolis, Rio de Janeiro

Enner Alcântara¹, José A. Marengo^{1,2}, José Mantovani¹, Luciana R. Londe^{1,2}, Rachel Lau Yu San³,
5 Edward Park³, Yunung Nina Lin⁴, Jingyu Wang³, Tatiana Mendes^{1,5}, Ana Paula Cunha^{1,2}, Luana
Pampuch^{1,5}, Marcelo Seluchi², Silvio Simões¹, Luz Adriana Cuartas^{1,2}, Demerval Goncalves², Klécia
Massi^{1,5}, Regina Alvalá^{1,2}, Osvaldo Moraes^{1,2}, Carlos Souza Filho⁶, Rodolfo Mendes^{1,2}, Carlos Nobre^{1,7}

¹Graduate Program in Natural Disasters, Unesp/Cemaden, São José dos Campos, Brazil

10 ²National Center for Monitoring and Early Warning of Natural Disasters (Cemaden), São José dos Campos, Brazil

³National Institute of Education, Earth Observatory of Singapore and Asian School of the Environment, Nanyang
Technological University (NTU), Singapore

⁴Institute of Earth Sciences, Academia Sinica, Taiwan

15 ⁵Institute of Science and Technology, São Paulo State University (Unesp), Department of Environmental Engineering, São
José dos Campos, Brazil

⁶University of Campinas, Institute of Geosciences (IG/Unicamp), Brazil

⁷Institute of Advanced Studies, University of São Paulo (IEA/USP), São Paulo, Brazil

Correspondence to: Enner Alcântara (enner.alcantara@unesp.br)

20

Abstract. On February 15, 2022, the city of Petrópolis in Rio de Janeiro, Brazil, received an unusually high volume of rain
within three hours (258 mm), generated by a strongly invigorated mesoscale convective system. It resulted in flash floods and
subsequent landslides that caused the deadliest landslide disaster recorded in Petrópolis, with 231 fatalities. In this paper, we
analyzed the root causes and the key triggering factors of this landslide disaster by assessing the spatial relationship of landslide
25 occurrence with various environmental factors. Rainfall data were retrieved from 1977 to 2022 (a combination of ground
weather stations and the Climate Hazards Group InfraRed Precipitation - CHIRPS). Remotely sensed data were used to map
the landslide scars, soil moisture, terrain attributes, line-of-sight displacement (land surface deformation), and urban sprawling
(1985-2020). The results showed that the average monthly rainfall for February 2022 was 200 mm, the heaviest recorded in
Petrópolis since 1932. Heavy rainfall was also recorded mostly in regions where the landslide occurred, according to analyses
30 of the rainfall spatial distribution. As for terrain, 23% of slopes between 45-60° had landslide occurrences and east-facing
slopes appeared to be the most conducive for landslides as they recorded landslide occurrences of about 9 to 11%. Regarding
the soil moisture, higher variability was found in the lower altitude (842 m) where the residential area is concentrated. Based
on our land deformation assessment, the area is geologically stable, and the landslide occurred only in the thin layer at the
surface. Out of the 1,700 buildings found in the region of interest, 1,021 are on the slope between 20 to 45° and about 60
35 houses were directly affected by the landslides. As such, we conclude that the heavy rainfall was not the only cause responsible

for the catastrophic event of February 15, 2022; a combination of unplanned urban growth on slopes between 45-60°, removal of vegetation, and the absence of inspection were also expressive driving forces of this disaster.

40 **1. Introduction and Background**

The municipality of Petrópolis is nestled in the mountains, 68 km from the city of Rio de Janeiro. It presents a rugged relief with numerous cliffs and it is populated by approximately 305,687 inhabitants. The city is predominantly urban¹ (95.1%) (Figure 1). It has been ravaged yet again by mudslides and floodings on February, 2022, when heavy rains triggered landslides
45 that left hundreds dead or missing. On that day, there was an unusually high amount of rain within three hours, amounting to 258 mm, as measured by rain gauges in the city. This was more than the prior 30 days accumulated rainfall and triggered the worst case of heavy rainfall in the city since 1932; this data was obtained by INMET (Brazilian Institute of Meteorology) using data from a rain gauge in Petrópolis (number 83804), which operates from October 01, 1912 to August 01, 1960. According to the National Center for Monitoring and Early Warning of Natural Disasters (Cemaden)², 250 mm of rain were recorded
50 between 4:20 pm and 7:20 pm, although the expected rainfall for the month of February would be 185 mm. The previous record had occurred in January 2011, with accumulated rainfall in order of 241.8 mm in 24 hours and a peak of 61.8 mm in one hour (Dourado et al 2012).

The abundant precipitation caused flash floods and mudslides in various sectors of the city, tearing down dozens of homes on the hillsides and causing floods in the streets. Images and videos on social media showed rivers of mud rushing through the
55 city's streets, sweeping away cars, trees, and people in its way. According to CNN³ and CPRM (2022), Brazil's Civil Defense Secretariat reported 269 landslides in this event. By the end of February, the death toll has risen to 231⁴.

While this is the deadliest flood and mudslide in the history of Petrópolis, heavy rains are not uncommon during Brazil's summer austral months (November to March; warm/rainy season).

According to Guerra et al (2005), Petrópolis was impacted by 1,161 catastrophic events between 1940 and 1990, which include
60 landslides, mudslides, rockfalls and floods. Most of these events were caused by torrential precipitation. The number of deaths appears to increase over time and nearly 90% of the events occurred within urban areas. Moreover, the human fatalities are also found to directly correlate with the spread of new urban settlements onto steep deforested hillsides. These disasters were responsible for the deaths of 526 people in the last 50 years, though seemingly worse over the last 20 years with 300 deaths. On February 5, 1988, a pouring rain fell on Petrópolis, which partially destroyed the city. This tragedy caused 171 deaths, left
65 more than 4 thousand people homeless, and thousands injured (Guerra et. al. 2005). On April 5, 2010, a precipitation in Rio

¹ IBGE: <https://cidades.ibge.gov.br/brasil/rj/petropolis/panorama>, last accessed on May 23, 2022

² www.cemaden.gov.br

³ <https://edition.cnn.com/2022/02/17/world/gallery/brazil-landslides/index.html>, last accessed on May 23, 2022

⁴ (<https://floodlist.com/america/brazil-floods-landslides-petropolis-february-2022>, last accessed on May 23 2022).

de Janeiro was the highest recorded in the past 30 years: weather stations recorded 288 mm within 24 hours, well over the average rainfall amount for April (140mm). It caused 52 fatalities in the city of Rio de Janeiro, and the total death count in the State was over 200. Approximately 160 others were injured and 15,000 had to leave their homes across the state. By the time the rain stopped, several days later, 12,000 people were homeless⁵.

70 The January 2011 disaster was, one with the highest impacts in the history of disasters in Brazil (Rosi et al 2019). With over 260 mm pouring down in less than 24 hours, the rain triggered a series of mudslides throughout the *região serrana* (mountainous region) northwest of Rio de Janeiro State, causing death and destruction in five nearby cities: Teresópolis, Petrópolis, Nova Friburgo, Sumidouro, and São José do Vale do Rio Preto. Nova Friburgo and Teresópolis each counted over 250 deaths with the final death toll of 900 and 300 still missing in the *região serrana*. In Teresópolis alone, 1,000 people were
75 left without homes (Rosi et al 2029) and claimed the lives of 73 people in Petrópolis (Marengo and Alves 2012). Such precipitation occurred because of the formation of an intense episode of rainfall generated by the action of the South Atlantic Convergence Zone (SACZ) that was intensified by a deep trough on the southeastern coast of Brazil. The SACZ is a typical meteorological system of the rainy season in the central area of Brazil, which normally develops between the months of November to March. The scale of the disaster brought attention to the rapid urbanization, infrastructure, and housing rights
80 issues within the context of disasters in Rio de Janeiro and Brazil, leading to the modernization of the Civil Defense structure in Brazil and the creation of CEMADEN.

Once again, on March 20, 2022, torrential rains caused flooding and landslides in the metropolitan area of Petrópolis and surrounding areas of the Mountain Region of the state of Rio de Janeiro⁶. Petrópolis Civil Defense reported 415 mm of rain in the São Sebastião district in just 10 hours, with 217.4 mm of that total falling in a 4-hour period between 14:00 and 18:00.

85 Around 100 incidents of landslides and flooding have been reported across the city, including flooded roads and buildings damaged or destroyed, and seven deaths linked.

The above examples demonstrated the adverse impacts of extreme weather and subsequent landslides on the people of Petrópolis and highlight the importance of assessing the causes of these landslides for future disaster management. Therefore, this study aims to better understand the main triggers for landslides and flash floods in Petrópolis, specifically for the disaster
90 in February 2022. To achieve this objective, we performed an integrated analysis of the urban sprawl over exposed areas, removal of vegetation and shallow saturated soil.

95

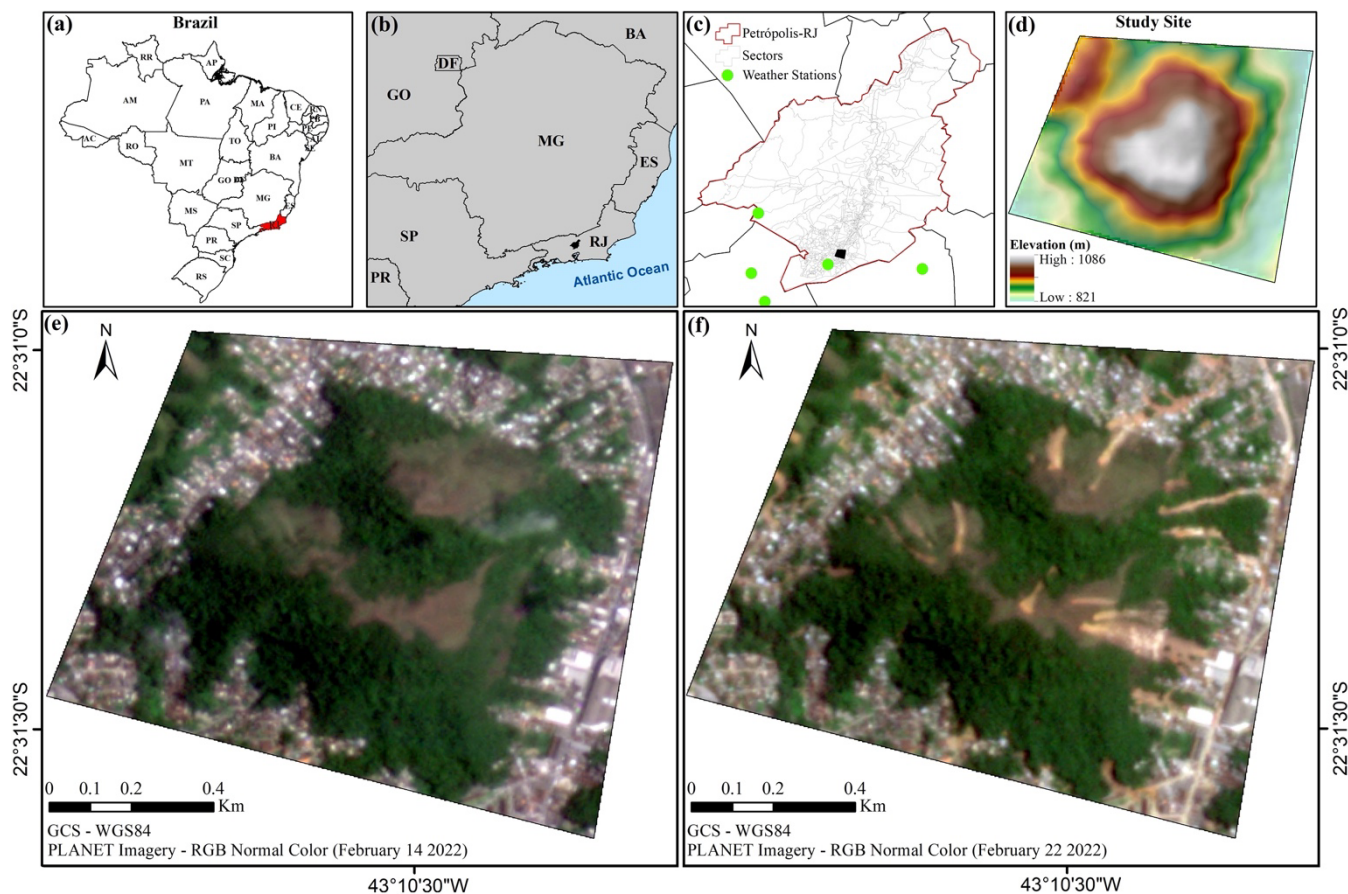
⁵ <https://www.france24.com/en/20100406-rio-de-janeiro-flooding-death-toll-passes-100>, last accessed on May 23, 2022

⁶ <https://floodlist.com/america/brazil-floods-landslides-petropolis-march-2022>, last accessed on April 20 2022

2. Data and Methods

2.1 Study Area

100 Petrópolis is located within the Atlantic Forest Biome, a biodiversity hotspot (Myers et al., 2000) (Figure 1). Currently, only 13% of the original cover remains (Fundação SOS Mata Atlântica/INPE, 2018), due to intense deforestation and human disturbance that mostly occurred in the first half of the 19th century (Dean, 1996). Historically, land degradation in the region is associated with a combination of different geomorphic processes, deforestation overexploitation (Nehren et al., 2019), and urban expansion (Guerra 1995, Rosi et al., 2019).



105 **Figure 1: Petrópolis and the study site. (a) location of Rio de Janeiro State in Brazil, (b) location of the study site in the Rio de Janeiro State. (a) – (b) were based on the Brazilian Institute of Geography and Statistics (IBGE). (c) location of the study site into Petrópolis city and the position of weather stations and (d) elevation map of the study site (ALOS/PALSAR, <https://asf.alaska.edu/data-sets/sar-data-sets/alos-palsar/>). (e) Planet image natural color from February 14, 2022, (f) Planet image natural color from February 22, 2022**

110

Petropolis is geologically located in the Rio Negro Complex, of paleoproterozoic origin, formed mainly by migmatites and granitoids. This part of Rio de Janeiro state suffered the effects of several regional metamorphic phases, resulting in highly foliated rocks cut by large ductile shear zones. These rocks are severely sectioned by fractures and faults of regional extension, with a strong reflection on topography since the entire region was submitted to tectonic events during the Precambrian period (IBGE 2018, Fonseca et al 1998, Penha et al 1981, Goncalves et al 1998, Rosi et al 2019). The drainage network of the region is strongly influenced by brittle regional structures, which play an essential role in its organization and the relief pattern and modeling. This set of geological characteristics, such as highly foliated and fractured rocks, trigger mass movements, mainly shallow landslides, and debris flow.

120 **2.2 Rainfall data and analysis**

To identify the extreme rainfall event in the municipality of Petrópolis on February 15, 2022, different precipitation datasets were retrieved from INMET and CEMADEN station data. CEMADEN has 17 rain gauges installed in Petrópolis, with measurements available from 2015 on, although some stations have a large amount of missing data for long periods, especially in the early years of the series. CEMADEN also has 5 Geotechnical stations, installed at the end of 2021, consisting of sensors that monitor rainfall and soil moisture at different depths (0.5 to 3.0m).

At the local scale, ground rain gauges provide direct-point estimations necessary for extreme rainfall analysis. However, a long precipitation time series is required for studying the extreme rainfall event in Petropolis. Since there is no single weather station with enough temporal coverage, rainfall data from five different weather stations located up to 15 kilometers from the highest accumulated rainfall location (Figure 1c) were considered. The hourly rain gauge observations from June 1976 to February 2022 were obtained from the Rio de Janeiro State Environmental Institute – Inea⁷ and the Cemaden⁸ databases.

While we initially considered using satellite-based products for studying rainfall, it proved to be inaccurate and thus, this approach was not carried on. Gridded data for global (Climate Hazards Group InfraRed Precipitation - CHIRPS, Funk et al., 2015) and regional domains (*Satellite-based Global Precipitation Measurement (GPM) - Integrated Multi-satellite Retrievals for GPM (IMERG) combined with data from surface observations – MERGE, from the Center for Weather Forecasts and Climate Studies – CPTEC, Rozante et al., 2010*) were found to exhibit poor capabilities in capturing the extreme rainfall event in Petrópolis (Huffman et al. 2020; Reis et al. 2020). Both products underestimated the storm-accumulated rainfall by 90% on February 15, 2022, throughout the study site. Previous studies have also shown that retrieving rainfall extremes from satellite-based products can present certain uncertainties concerning accuracy probability due to instrument issues and retrieval algorithms or the interpolation process (Jiang et al., 2019; Dembélé and Zwart 2016; Hermance and Sulieman, 2018).

To examine the synoptic weather pattern that spawned the mesoscale convective system (MCS) with unprecedented torrential rainfall, the fifth generation of atmospheric reanalysis (ERA5) produced by European Centre for Medium-Range Weather

⁷ <http://www.inea.rj.gov.br/ar-agua-e-solo/monitoramento-hidrometeorologico/>

⁸ <https://www.gov.br/cemaden/pt-br>

Forecasts (ECMWF; Hersbach et al., 2020) is adopted for the analysis of atmospheric environment. ERA5 features a horizontal resolution of 31 km and 137 vertical levels with hourly output frequency, which provides a detailed picture of the MCS-hatching synoptic background. Meanwhile, the morphology and organization of high precipitation MCS is analyzed using the
145 National Aeronautics and Space Administration (NASA) merged geostationary satellite half-hourly 4-km-resolution Infrared brightness temperature data (Merged IR; Janowiak et al., 2017).

2.3 Terrain Analysis using DEM

150 The terrain morphology of Petrópolis could have also influenced the slope stability (Costanzo et al., 2012), causing certain areas to be more susceptible to landslides than others. Terrain attributes widely used in landslide susceptibility assessments include elevation, slope angle, aspect, and curvature (Catani et al., 2013; Chen et al., 2017; Reichenbach et al., 2018; Dias et al., 2021). Different elevation creates diverse environmental conditions in temperature, rainfall regimes and vegetation (Dai and Lee, 2002; Costanzo et al., 2012; Catani et al., 2013) which also influence human development (Chau and Chan, 2005).
155 Slope angle affects the shear stress acting on the slope and has been considered one of the biggest determinants for landslide occurrences (Rodríguez et al., 2008; Catani et al., 2013; Kanwal et al., 2017). Slope aspect refers to the direction of a slope and determines sunlight exposure, often correlating with moisture retention and vegetation cover and consequently landslide initiation (Guzzetti et al., 1999; Dai and Lee 2002; Rodríguez et al., 2008). Slope curvature is the rate of change of the slope, and this controls the direction of landslide motion by concentrating or dispersing surface runoff and gravitational stresses
160 (Ohlmacher, 2007; Costanzo et al., 2012).

To assess the effects of terrain morphology on this landslide event, the digital elevation model (DEM) was obtained from ALOS PALSAR, available at the Alaska Satellite Facility (ASF). ALOS/PALSAR images were resampled (cubic interpolation) from 30 m to 12.5 m pixel size with orthometric altitude (EGM96 geoid model) before being converted to a geometrical altitude (ellipsoidal). The following terrain attributes were derived from the DEM: slope angle, slope aspect, and
165 slope curvature.

The spatial variation of the three slope attributes within this landslide extent was assessed. The slope angle was classified into five classes: 0°-15°, 15°-25°, 25°-35°, 35°-45°, and 45°-60°. Slope aspect was categorized into classes of 45°, corresponding to Flat (-1), N (0°-22.5° and 337.5°-360°), NE (22.5°-67.5°), E (67.5°-112.5°), SE (112.5°-157.5°), S (157.5°-202.5°), SW (202.5°-247.5°), W (247.5°-292.5°), and NW(292.5°-337.5°). Slope curvature was reclassified into 3 categories – upwardly
170 convex (negative), flat (zero), and upwardly concave (positive). To account for the slope morphology of the entire study area, the landslide extent within each class of slope angle, aspect, and curvature was calculated in terms of proportion to the study area.

175

2.4 Optical remote sensing data and soil moisture pattern

180 Soil moisture was analyzed through images from the Operational Land Imager (OLI) and the Thermal Infrared Sensor (TIRS) on board of the Landsat-8 and 9 satellites. Images from the Planet satellites were also selected (see Table 1). Images from Landsat satellites are surface reflectance products at 30-m resolution, which were obtained from the USGS Earth Explorer site⁹. The Planet constellation consists of more than 130 orbital Earth observation satellites acquiring daily images of the Earth on four bands in the visible and near infrared wavelength range at 3-0 m spatial resolution.

Table 1: Satellite imagery used in this study.

Sensor/Satellite	Date
OLI and TIRS/Landsat-8	Jan, 28 2021
OLI and TIRS/Landsat-8	Mar, 17 2021
OLI and TIRS/Landsat-8	Apr, 02 2021
OLI and TIRS/Landsat-8	July, 07 2021
OLI and TIRS/Landsat-8	July, 23 2021
OLI and TIRS/Landsat-8	Aug, 24 2021
OLI and TIRS/Landsat-8	Sep, 09 2021
OLI-2 and TIRS-2/Landsat-9	Jan, 23 2022
Planet	Feb, 14 2022
Planet	Feb, 22 2022

185

The Soil Moisture Index (SMI, Lambin and Ehrlich, 1996; Zhan et al., 2004) was used to reconstruct the dynamics of soil moisture from 2021 to the beginning of 2022. This index can be estimated from Land Surface Temperature (LST) and Normalized Difference Vegetation Index (NDVI). According to Lambin and Ehrlich (1996), the scatterplot of LST vs NDVI results in a trapezoidal shape, and all types of land cover fall within the trapezoid of the LST-NDVI space. The upper envelope of the trapezoid (upper limit of surface temperature for a given vegetation cover) represents the dry condition (warm edge), while the lower limit represents the wet condition (cold edge) (Parida et al., 2008).

190

Landsat-8 and 9 images were used to calculate the SMI. OLI/Landsat-8 and 9, Level-2 satellite images were obtained at the USGS Earth Explorer website¹⁰ from 2021 to 2022. Level-2 data is atmospherically corrected and generated from the LASRC (Landsat-8 Surface Reflectance Code), that yields surface reflectance at a 30-m spatial resolution suitable for studying the dynamics of our study site (Silva et al. 2021). OLI images were used to calculate the NDVI whereas TIRS/Landsat-8 and 9 were used to calculate LST. SMI values, at a range between 0 (drier soil) and 1 (wet soil), are calculated according to Zhan et al., (2004):

195

200

$$SMI = \frac{LST_{max} - LST}{LST_{max} - LST_{min}} \quad (1)$$

⁹ <https://earthexplorer.usgs.gov>

¹⁰ (<https://earthexplorer.usgs.gov>)

where, LST_{max} and LST_{min} are, respectively, the maximum and minimum values of LST within the image for a given NDVI, expressed as:

$$205 \quad LST_{max} = a_1 \times NDVI + b_1 \quad (2)$$

$$LST_{min} = a_2 \times NDVI + b_2 \quad (3)$$

210 where, a and b are empirical parameters defining the dry and wet edges modeled as a linear fit to the data (Zhan et al., 2004; Parida et al., 2008; Potić et al., 2017).

2.5 Interferometric Synthetic Aperture Radar (InSAR) analysis of ground deformation

215 Ground deformation was studied using multi-temporal interferometric synthetic aperture radar (MTInSAR) time-series analysis. C-band Sentinel-1B SAR data of descending path 155 acquired between 8 May 2015 and 20 December 2021 were collected and processed in InSAR Scientific Computing Environment (ISCE) to form a coregistered stack of single look
220 complex (SLC) images. No new images were acquired between December 21, 2021, and February 22, 2022 due to the Sentinel-1B anomaly, meaning that there is no data acquired right before and after the landslides in mid-February 2022. The coregistered SLC stack is then processed in Fine Resolution InSAR using Generalized Eigenvectors (FRInGE, Fattahi et al., 2019) to form a wrapped phase time-series via a phase linking approach (Ansari et al., 2018), which is then unwrapped epoch-by-epoch using
225 SNAPHU to generate the final displacement time-series (Chen and Zebker, 2001). Tropospheric correction is carried out on the displacement time-series using the ERA5 weather model (Jolivet et al., 2014). Line-of-sight (LOS) velocities and velocity errors are then estimated using the L1-norm iterative reweighted least squares algorithm (Schlossmacher 1973).

2.6 Mapping urban sprawling and forest losses

225 The urban sprawl analysis was performed using data available at the MapBiomas Project - Collection 6¹¹, with spatial resolution at 30 meters. The MapBiomas Project provides a historical series of land use and land cover (LULC) information and the transition data between 1985 and 2020 to the whole country, based on random forest algorithm applied to Landsat archive using Google Earth Engine (Souza et al., 2020). The LULC data of eight years (1985, 1990, 1995, 2000, 2005, 2010, 2015, and 2020) were analyzed focusing on the urban area and forest formation classes to observe the growth of occupation in
230 the Petropolis municipality and the area of interest (AOI, see Figure 1f). Urban sprawl and loss of vegetation (suppressed forest) were visual and quantitatively analyzed through the transition data for seven five-year periods, from 1985 to 2020.

2.7 Deriving the landslide scars map

235 The building footprints were compared to landslide scars to quantify either impacted or destroyed buildings as a consequence of this event. Moreover, these building footprints were confronted with the slope data to obtain the slope range they occupy on the hill. The building footprints were obtained by OpenStreetMap (OSM) database. The OSM is a crowdsourced mapping

¹¹ <http://mapbiomas.org>

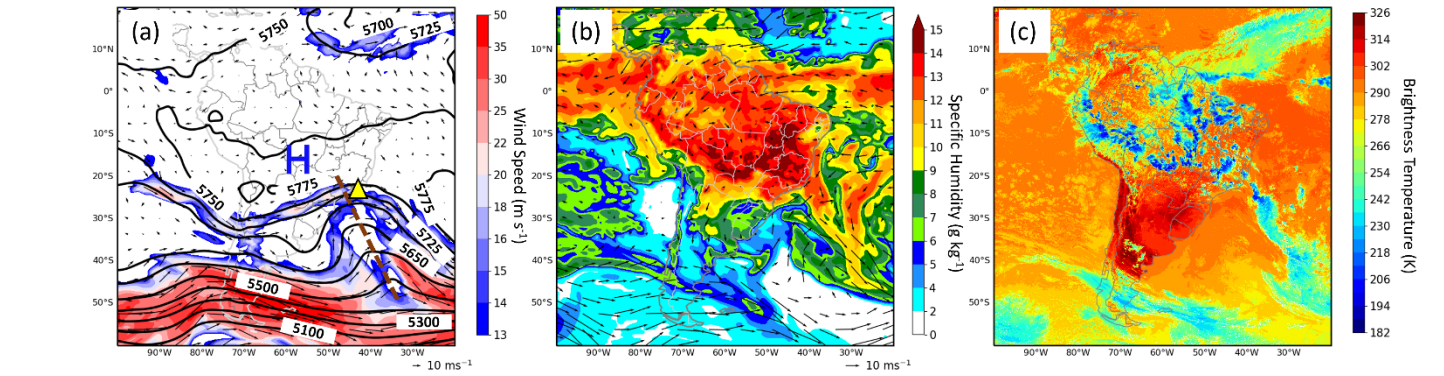
project that aims to create and provide a freely available geographical information database of the world (Goldblatt et al., 2020; Minghini and Frassinelli, 2019). The mapping of this area was performed as an urgent project after the event on February 17, which resulted in flooding and landslides in several parts of the municipality.

240

3. Results

3.1 Synoptic background analysis

Right before the onset of record-breaking rainfall, central Brazil was dominated by a wide-spread subtropical high-pressure center at 500 hPa level (Figure 2a), whose southern boundary pushed to the 22°S parallel above Petrópolis. As revealed in many previous studies (e.g., Maddox et al. 1978; Mitchell et al. 1995; Wang et al., 2019b), the atmosphere directly under the subtropical high-pressure center is most stable because a subsidence inversion layer (capping inversion) is formed as a result of widespread descending air. However, the atmosphere becomes more unstable toward the edge of the high pressure because of the weakening inversion, which promotes the occurrence of convection. Consequently, a ring of precipitation area commonly forms at the periphery of the high pressure, known as a “ring of fire” pattern (Galarneau and Bosart 2006). The 850 hPa specific humidity distribution (Figure 2b) echoes this pattern, as the warm and moist air is being pushed southeastward towards the edge of the subtropical high, and the moisture is further advected to Petrópolis which fuels the convection there. Figure 2c exhibits the concurrent cloud distribution, where the cold colors (< 241K) represent the presence of deep clouds whose cloud top temperature is cooler than the surrounding area without clouds, and A MCS is formed over Petrópolis. In addition to the influence of the high-pressure center, the MCS that affects Petrópolis is further intensified by a long-wave trough as indicated in Figure 2a. The city is located to the bottom of the 500 hPa trough where there is a strong lifting of air that facilitates the intensification of convection. In summary, the edge of a subtropical high intersects with a long-wave trough over Petrópolis, forming a very favorable environment for the occurrence of high precipitation MCS, which later produced the unprecedented torrential rainfall that caused the flood and landslide.



260 **Figure 2: Large-scale environmental variables and satellite observation at 16:00 (local time). (a) wind speed (shading), geopotential height (contour), and winds (arrow) at 500 hPa, where the trough line is indicated using a brown dash line**

and the location of Petrópolis is highlighted by a yellow triangle. (b) Specific humidity (shading) and winds (arrow) at 850 hPa. (c) Merged IR brightness temperature, where cold color represents the presence of deep clouds.

265 3.1 Rainfall spatiotemporal variability

Figure 3 shows the January-February daily rainfall distribution from 1977 to 2022. By comparing the shape of the boxplot for 2022 with the other years, the third quartile of 2022 was observed to be the biggest of the entire series (22.35mm). It indicates that in January and February 2022, 25% of the days accumulated daily precipitation higher than 22.35 mm. 2022 also registered 3 outliers (circles). Compared with the other years, this number is not so expressive, but the records stand out for being abnormally high (rainfall accumulated of 88.8 mm, 219.6 mm and 260 mm in one day). In 2022, the most intense outliers were also higher than in all other years of the series (only 4 events greater than 189.6 mm) (Figure 3). The value registered on February 15, 2022 (260 mm) is the second largest value for that month in the 46-years series.

270 An intense rainfall, starting on the evening of February 15, 2022, caused mudslides on the hillsides above downtown Petrópolis and produced flooding that did more damage in the streets below. Images and videos on social media showed rivers of mud rushing through the city's streets, sweeping everything along the way: cars, buses, trees, and sometimes people. Petrópolis recorded 252.8 mm of rain in just 3 hours on February 15 (São Sebastião station - 330390604G) (Locations 1 and 2 in Figure 5). The average for the entire month of February is approximately 200 mm. Landslides and flooding events in Rio de Janeiro happen most frequently during the rainy season (from December to April austral summer). Such hourly rates and amounts have not been recorded in Brazil and are rare even for other parts of the world.

280

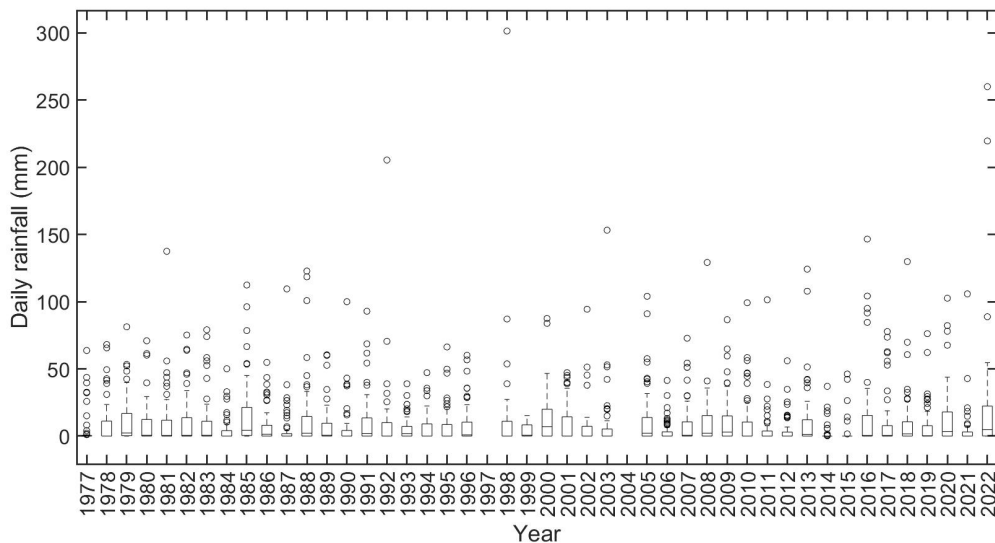
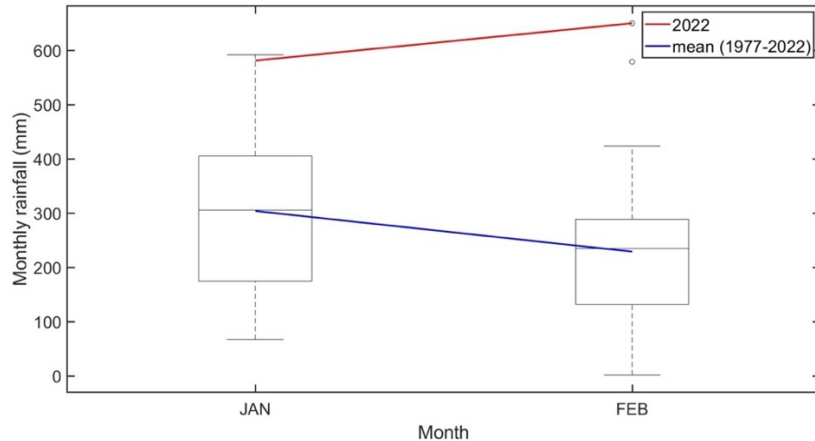


Figure 3: The Long-Term precipitation time-series was created from 2 weather stations from INMET (A603-Duque de Caxias and A610-Pico do Couto), 2 weather stations from INEA (2243238-Xeren and 2243235-Andorinhas), and one from Cemaden (Sao Sebastiao).

From our results, the mean precipitation for the region in January is 304.19 mm, while in February it is 229.28 mm (Figure 4). January 2022 registered an accumulated rainfall of 581.4mm, the second biggest value in entire series. In February, the accumulation was 650mm, the largest value for the 46-years series and considered as outlier for the month (circle).

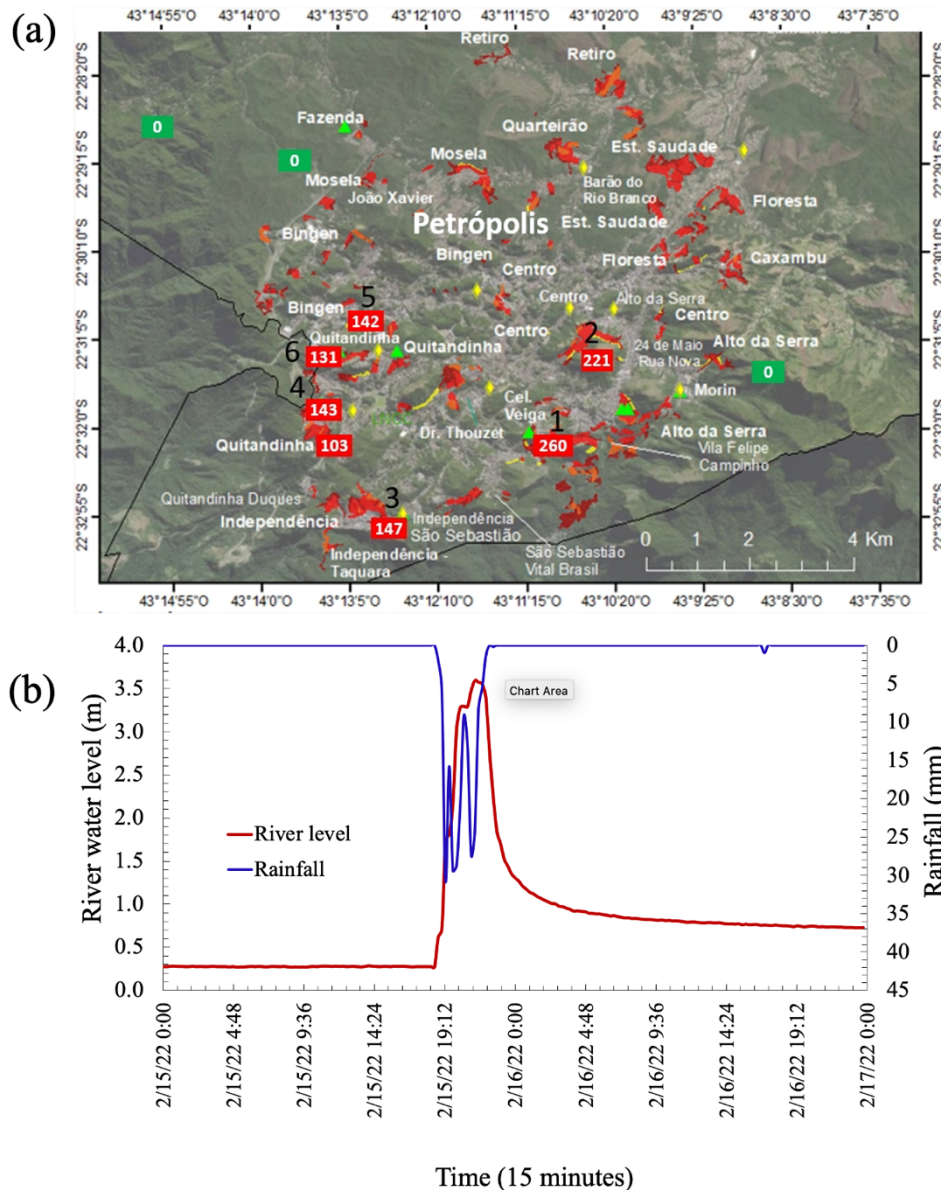


290

Figure 4: January and February rainfall (mm) distribution (boxplot) for 1977-2022. Blue line indicates the mean value for 1977-2022 period (for the months of January and February) and red line represents the accumulated rainfall for 2022. Circles represents outliers.

295

For the February 15, 2022, event, Figure 4a depicts the station-based 24-h rainfall accumulated over Petrópolis. The highest rainfall accumulation was observed at São Sebastião station (330390604G), flagged as “1” in Figure 5.



300 Figure 5: (a) Accumulated precipitation in 24-hours on February 15, 2022 at CEMADEN rain gauges. Red contours
 correspond to areas of risk for landslides at Petrópolis. The black line indicates the municipality limit. The cartographic
 base was obtained from ©OpenStreetMap contributors 2022. Distributed under the Open Data Commons Open
 Database License (ODbL) v1.0. (b) Rainfall (blue) and river level (red) time series for February 15, 2022 time event, at
 305 Alto da Serra hydrological station (INEA).

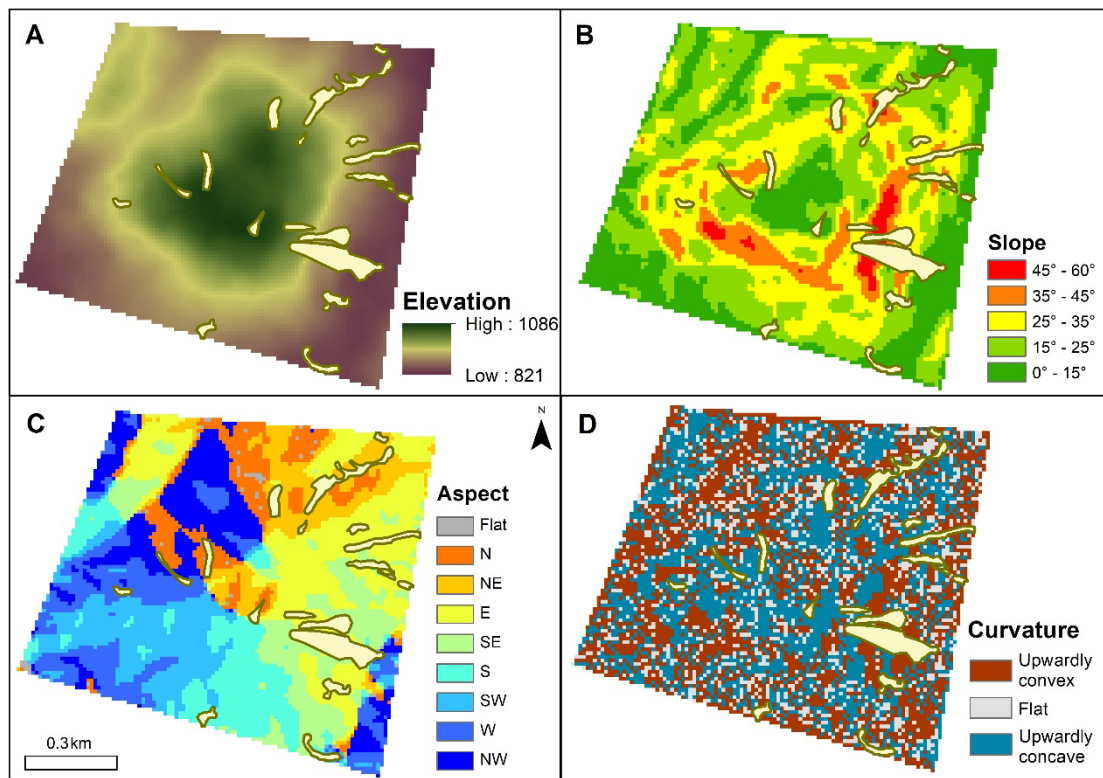
It recorded about 260 mm in 24-h and approximately 230 mm in two 3-h intervals from 16:00 to 21:00 (local time). Another nearby station - Dr. Thouzet (330390603G) - also registered 221 mm in 24-h (flagged as “2” in Figure 4). Station Independencia2 (330390612A), Quitandinha (330390601G), 143 mm (“4” in Figure 4), Bingen (30390605G), 142 mm (“5” in

310 Figure 4) and Rua Amazonas/Quitandinha (330390618A), 131 mm (“6” in Figure 4). The INEA hydrological station, Alto da
Serra (2243315) was the only one with abaixable data for this event. The peak level was 3.59 m (Figure 4b) for an accumulated
rainfall of 207 mm until the peak (the total rainfall was 223 mm). The maximum peak previously registered was 2.58 m on
March 18, 2013 (data period 2012 – 2021), for an accumulated rainfall of 186 mm. It is noteworthy that a heavy precipitation
particularly affected the urban part of the city, where risk areas are located. Further away, over the rural part of the municipality,
no rainfall was recorded.

315

3.2 Characterization of the terrain to assess landslide susceptibility

Located in the mountainous regions, Petrópolis is in a relatively high elevation. Its average elevation is 953.5 m across the
study extent, and it ranges from 821 to 1086 m (Figure 6A).



320

Figure 6. Distribution map of terrain attributes in the study area of Petrópolis. (A) Elevation (B) Slope (C) Aspect and (D) Curvature of Petrópolis. Light yellow polygons represent the extent of the February 2022 landslide patches.

325

Although the landslide scars were found across all elevations, most of them began above 950 m elevation. As for the slope morphology, the highest slope angle recorded in this study area is approximately 60° (Figure 6B), the east-facing slopes account for the largest area (Figure 6C) and most of the slopes were either concave or convex (Figure 6D). Spatial analysis revealed that, out of the 5 categories of slope angles, slope angles of 45-60° had the highest percentage of landslide occurrence with 23% (Figure 7A). There was also a distinct increasing trend in the proportion of landslide occurrences as the slope becomes steeper. This corresponds to numerous previous findings that steeper slopes increase slope instability due to greater resistance required to maintain stability (Rodríguez et al., 2008; Catani et al., 2013; Reichenbach et al., 2018). It is often one of the most important factors when assessing landslide susceptibility (Costanzo et al., 2012; Reichenbach et al., 2018). However, complementary analysis is required for the occurrence of landslides in slopes lower than 25°, as they may be associated with the execution of slopes of cuts and/or fills (Ávila et al., 2021; Mendes et al., 2018a; Mendes et al., 2018b).

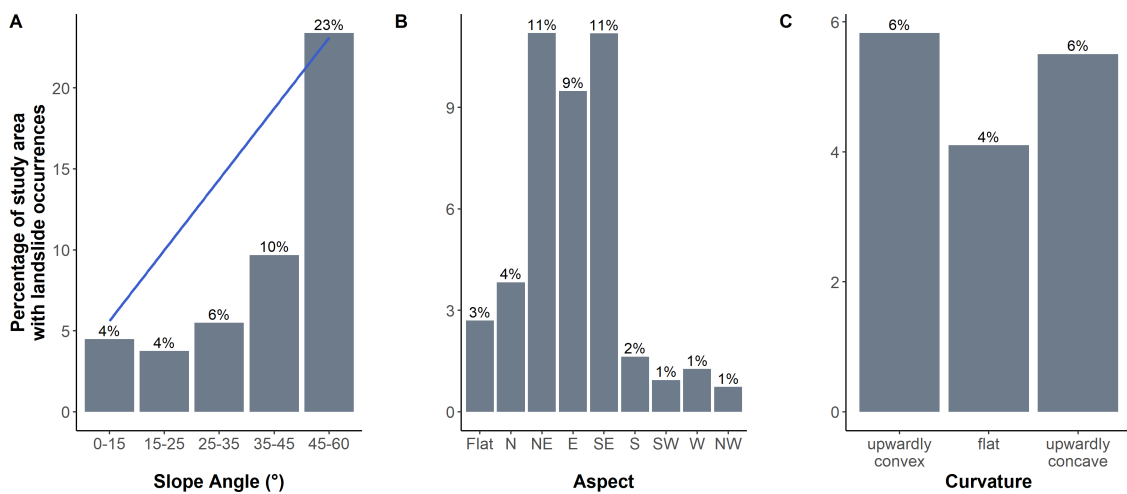


Figure 7. Percentage of the landslide area in relation to the total study area, in each classification of A: Slope (blue trend line); B: Aspect, C: Curvature.

340

For the aspect factor, the east-facing slopes appear to be the most conducive for landslides, as they account for more than 30% of landslide occurrences (Figure 7B). Conversely, west-facing slopes had the lowest landslide occurrence with only 1% experiencing landslides. This could be attributed to multiple reasons such as the exposure of the surface to varying extents of wind and solar radiation prior to the landslide event (Guzzetti et al., 1999; Dai and Lee, 2002). This could have conditioned the soil moisture, humidity, as well as vegetation growth on the slopes (Catani et al., 2013; Reichenbach et al., 2018). Vegetation growth in Petrópolis was observed to be more abundant on west-facing slopes, which could have increased the slope stability in that direction due to their extensive root systems. Additionally, the rainfall direction during the storm could have also favored landslides in the eastward orientation.

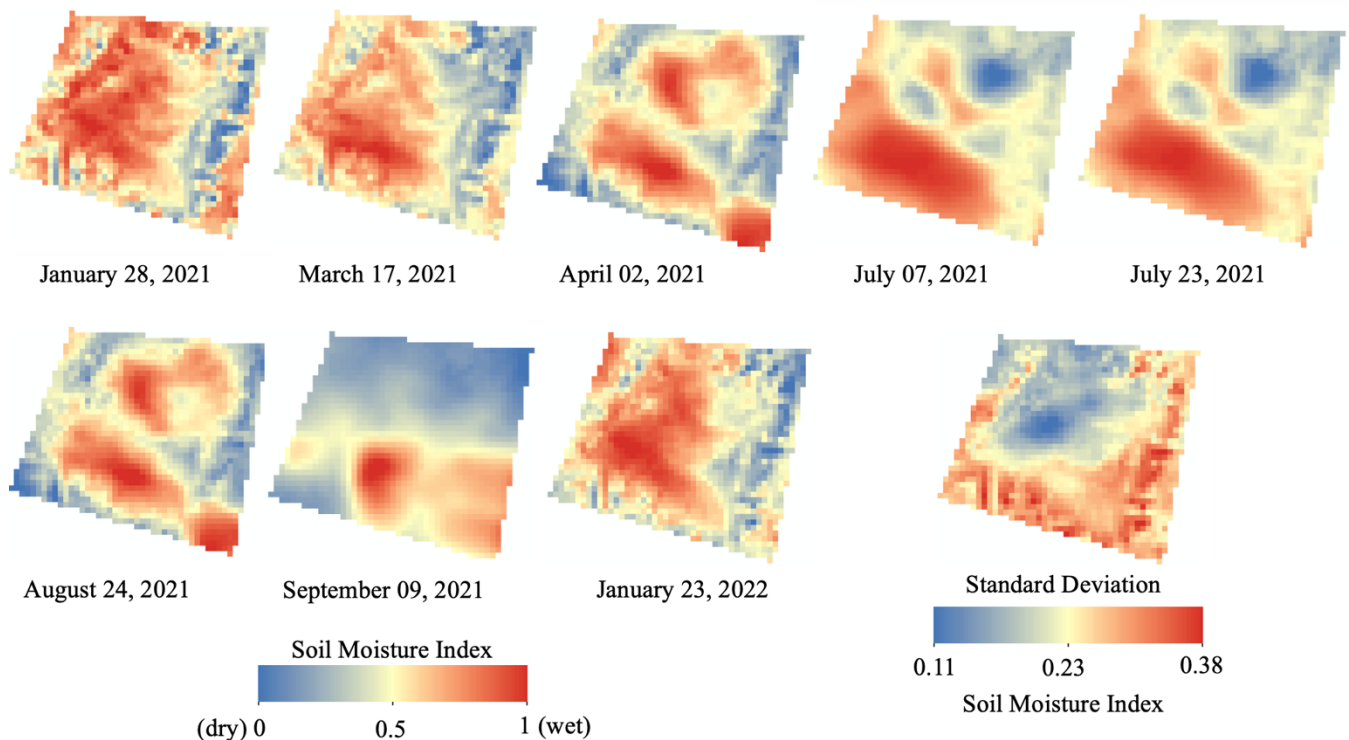
345

350 In terms of slope curvature, these landslides did not appear to vary substantially between the different curvatures (Figure 7C).
While upwardly convex (negative curvature) and concave (positive curvature) slopes (6%) had a higher percentage of landslide
occurrences than flat curvatures (4%), the difference is small at about 2%. Based on the spatial analysis of the terrain
morphology, this Petrópolis landslide event was likely associated with the terrain morphology of the mountain even though
the trigger was induced by the intensive rainfall during the storm.

355

3.3 Soil Moisture trend prior to the landslides

The estimations of SMI from January 2021 to January 2022 are shown in Figure 8. Values near zero represent dry soil
conditions and values near 1 mean wet soil conditions. The results shows that the wet soil conditions were more frequently in
the highest altitude and dryer in the lower altitude during the summer from January 2021 to April 2021 (Compare with Figure
360 6A for elevation). The soil moisture becomes higher in the south portion during the winter (July to September 2021), mainly
in the lower altitude, with one exception in August, when it resembles the summer pattern. In January 2022, the moisture
condition spread throughout the area, just like in January 2021. The spatial standard deviation image showed a higher
variability in lower altitude than in higher altitude. The main concentration of buildings within our study site was also found
within the region with higher moisture variability.



365

Figure 8: Soil moisture index from January 28, 2021 to January 23, 2022.

370 **3.4 Interferometric synthetic aperture radar time-series**

InSAR time-series analysis revealed a narrow zone on the eastern slope of the study site with a continuous motion away from the satellite at a rate of 2-3 mm/year (Fig. 9C). Given the line-of-sight (LOS) direction, the motion can be either westward or downward. Since westward motion is nearly impossible on an east-facing slope, we interpreted the motion as a continuous down-slope movement with part of the downward motion (negative LOS velocity) canceled by the eastward motion (positive LOS velocity).

375 LOS velocity).

This interpretation means that the actual down-slope velocity needs to be larger than the LOS velocity. Considering the slope angle (about 50°-60°; see Figure 6) and the satellite angle (about 38°), the actual down-slope velocity within this zone can reach as high as 10-15 mm/year. Other than this zone, the rest of the study site showed little ground deformation between May 2015 and December 2021.

380

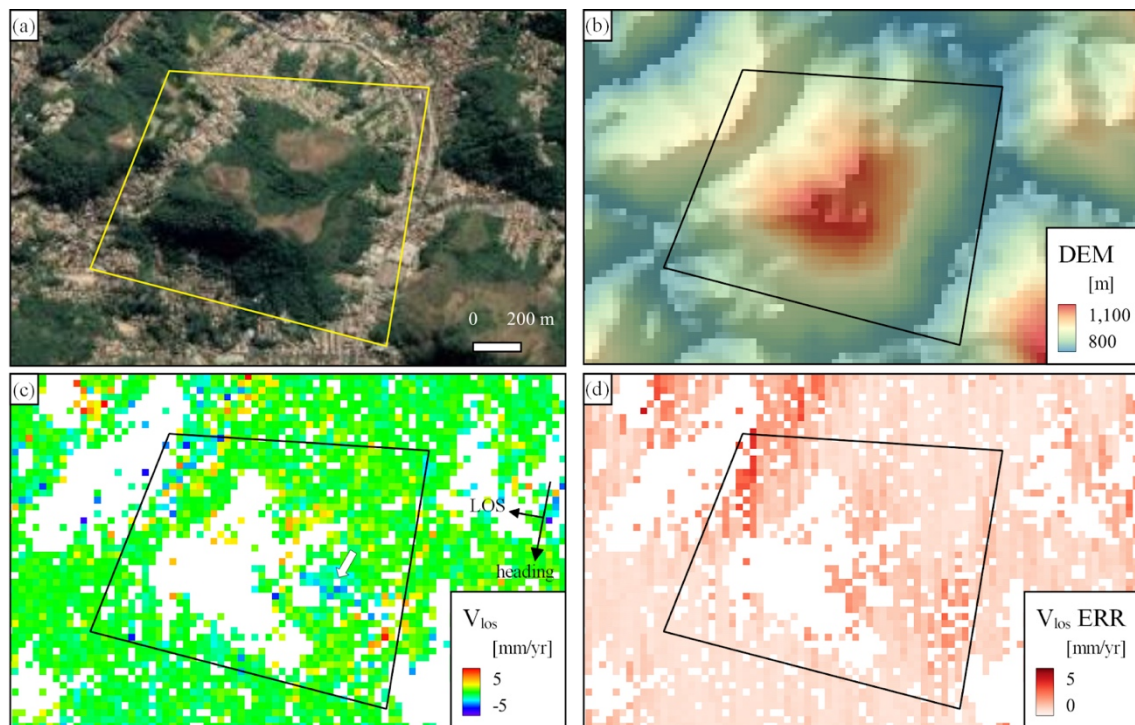


Figure 9: (A) Optical image before February 2022 landslides (Image from Google Earth Pro). (B) Digital Elevation Map (ALOS/PALSAR). (C) InSAR line-of-sight (LOS) velocity between May 8, 2015 and December 20, 2021. Note that most areas have nearly zero deformation except for the eastern slope (pointed by a white arrow). (D) Standard deviation of LOS velocity.

385

3.5 Urban sprawling, forest losses and landslides scars

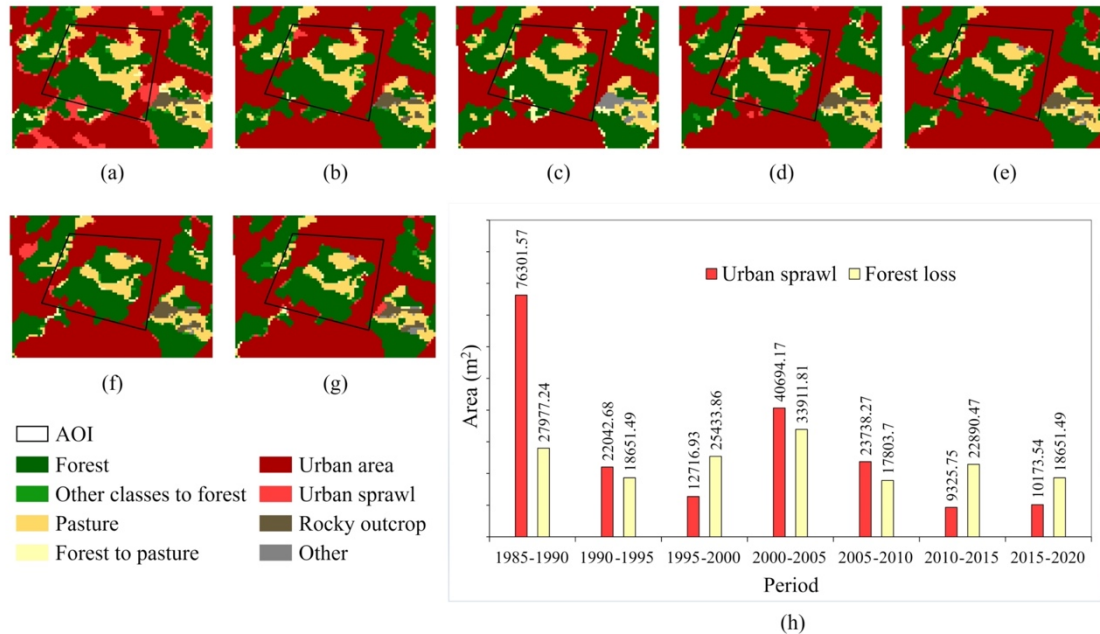
390 During the last 35 years, forest formation in the municipality of Petrópolis has been increasing (7.08%: from 410.55 to 439.64
km²) and urban areas have largely expanded (58.78%: from 32.07 to 50.93 km²), while pasture and agriculture have lost cover
(14.73%: from 336.70 to 287.09 km²). However, when analyzing in a five-year interval, forest cover has mostly increased
395 from 1985-2010 (Table 2: there was a small decrease from 1995-2000). Since 2010, though, there has been a loss of 1.50% in
vegetation cover (6.72 km²). Pasture and agriculture have been consistently decreasing during the study interval (exceptions
were 1995-2000 and 2010-2015; Table 2). Regarding urban areas, 1985 to 1990 was the period with the highest increase (about
22%), and the urban expansion stayed at a constant rate of 2-7% since then, accruing to a total increase of 58% in 35 years.

Table 2. Percentage of change in LULC classes over 5-year periods for the Petrópolis municipality

Period	Forest	Urban area	Rocky outcrop	Pasture and agriculture	Other
1985-1990	3.54	22.45	-0.37	-6.39	-13.53
1990-1995	3.00	7.04	0.70	-4.97	-13.05
1995-2000	-0.72	4.83	-0.35	0.43	-9.74
2000-2005	0.84	4.16	1.81	-2.06	10.64
2005-2010	1.81	2.48	2.80	-3.47	23.03
2010-2015	-1.46	4.38	2.14	1.22	28.63
2015-2020	-0.04	3.69	-2.92	-0.26	21.74

400

In Petrópolis municipality, forest cover has historically been replaced mostly by pasture and agriculture (3.38%), followed by urbanization (0.77%). Looking closer to the study area, forest loss has been constant all over the study interval, reaching about 16.6 ha by 2020 (Figure 10 and Table 3). When the urban expansion data for the study area is observed (Fig. 10 and Table 3),
405 it is verified that this study area reflects the data presented for the municipality, with an increase in the urban area over the periods and a higher urban expansion for the period of 1985 to 1990. The urban sprawl can be seen in Figure 10, which presents the transition information between classes for the study area.



410 **Figure 10. Transition classes for the study area: (A) 1985 – 1990, (B) 1990 – 1995, (C) 1995 – 2000, (D) 2000 – 2005, (E) 2005 – 2010, (F) 2010 – 2015, (G) 2015 – 2020 and (H) area (m²) of urban sprawl and forest loss over the analyzed period.**

Table 3. Urban sprawl and forest loss classes in the area of interest.

Period	Urban sprawl (m ²)	Forest loss (m ²)
1985-1990	76301.57	27977.24
1990-1995	22042.68	18651.49
1995-2000	12716.93	25433.86
2000-2005	40694.17	33911.81
2005-2010	23738.27	17803.70
2010-2015	9325.75	22890.47
2015-2020	10173.54	18651.49

415 For the study area, approximately 1700 buildings that occupy the area around the hill were counted. When the buildings were confronted with landslide scars, it was found that at least 60 houses were affected by landslides. Due to the characteristics of the relief in the region, occupation on hillside areas is very common. Most of them (1021 buildings) are on the slope range of 20 to 45% (Figure 11). It was observed that 343 buildings occupy areas with slopes above 45%, which are considered

Permanent Preservation Areas, according to the Brazilian Environmental Legislations (Law nº 12.651/2012) (Brasil, 2012).

420 Considering the use and occupation of the study area, further stability analysis is recommended to verify the possibility of variation in the safety factor of the slopes due to the execution of slopes of cuts and fills (Mendes et al., 2018a; Mendes et al., 2018b).

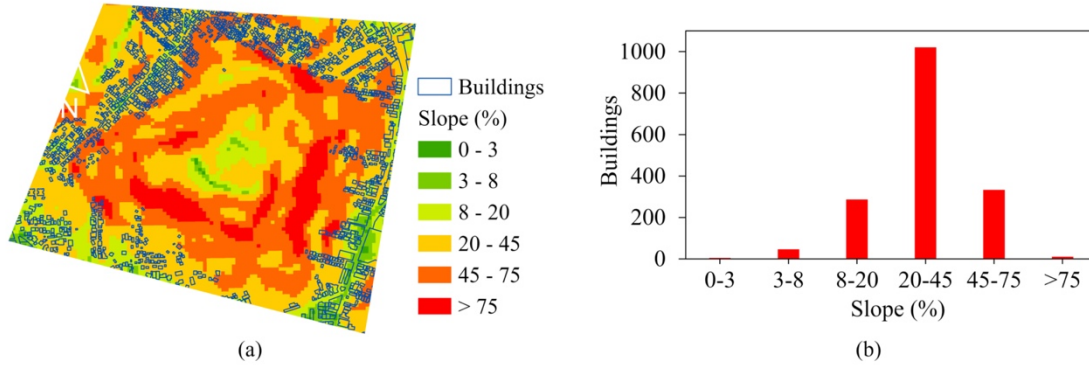
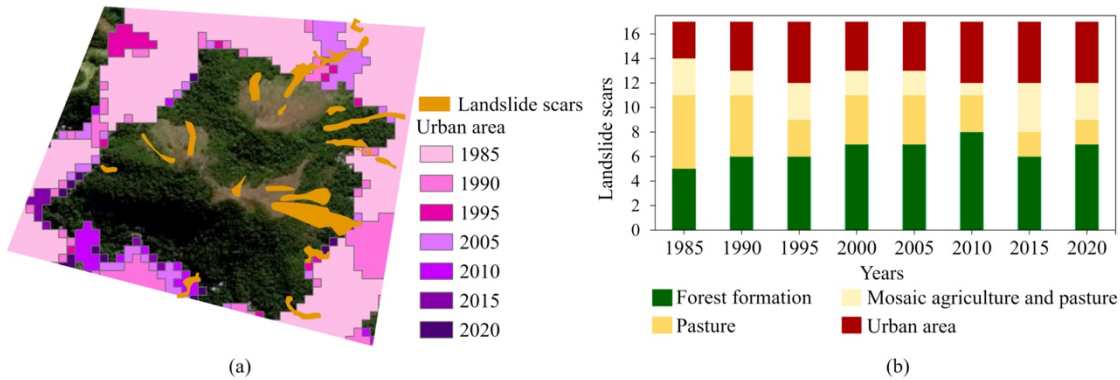


Figure 11: Building footprints and slope in the area of interest (A) and (B) number of buildings per slope intervals.

425 The landslide area coinciding with the urban area totaled about 17,000 m² (Figure 12A). The scars occurred in areas of forested area, urban area, pasture and agriculture, common classes in the urban region of the municipality. From the zonal statistics considering the landslide scars of this event and the LULC class as the majority in its interior, it was verified that there were lesser landslide scars on urban areas in 1985, compared to the years after. Over the years, more scars were found with urban area predominancy, and fewer scars were found on agriculture and pasture. This finding may be an indication that urban sprawl

430 at the beginning of the analysis period (1985) is sufficient for landslides to cause destruction, material damage, and loss of life in the region. The graph in Figure 12b shows the zonal statistic result for the 17 landslide scars (2022-year event) and LULC classes for the years of analysis.



435

Figure 12: (A) Landslide scars superimposed in the urban area classes (the background image is from Planet) and (B) zonal statistics based on LULC classes (for every 5 years, from 1985 to 2020).

440

4. Discussion

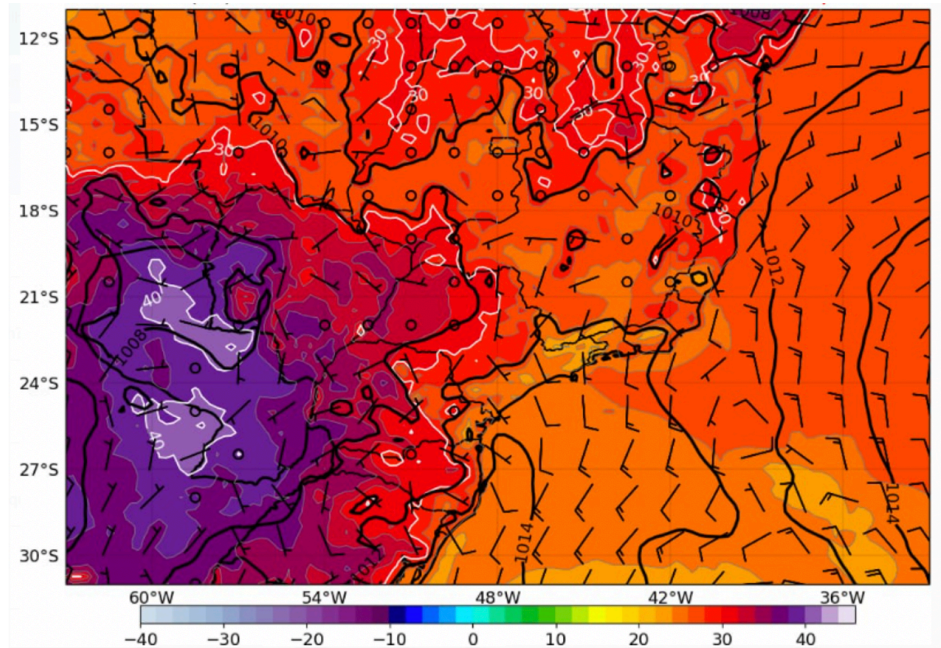
4.1. Origin/Cause of the extreme rainfall, subsequent flood and landslide

The weather forecasts issued by INMET and CEMADEN for the mountainous region of Rio de Janeiro, released earlier on February 14th, warned about isolated convective rainfall, which could occur in some areas of the city. However, no meteorological model predicted such significant amounts of rainfall over the region. The heavy rainfall that occurred in the city of Petrópolis on February 15th was caused by the action of a meteorological phenomenon known as mesoscale convective cell, with extraordinary characteristics without known recorded antecedents. The situation was influenced by the presence of the South Atlantic Convergence Zone (SACZ), that at the time was positioned over the state of Rio de Janeiro and created a favorable environment for atmospheric convection.

The other key element that led to the extraordinary rains in the center of Petrópolis was the passage of a cold front, with very particular characteristics, which occurred at the exact moment when the rain showers began to form over the city. This cold front, on the one hand, was weak to dissipate the instability related to the storm clouds and, on the other hand, it was strong enough to change the wind direction, which came from the south, exactly perpendicular to the Petrópolis mountain range. As a result of this combination of factors, the mesoscale convective cell cloud (technically called of cumulonimbus), which should have lasted a few minutes, lasted several hours due to the interaction of the southerly winds associated with the cold front in the mountain. Figure 13 shows the surface winds and temperature for the 18:00 UTC on February 15th. It is noticed the cold front with the temperature gradient and changes in wind direction. Southerly winds on the mountain region where the urban part of the of the city of Petrópolis (region prone to landslides) turned the "orographic cloud" (cloud that positions on the top of mountains for hours and that normally do not precipitate) into a convective cell, which is very rare. Due to the sudden formation and the null displacement of the storm, the weather radars also did not allow its anticipated tracking. It is noteworthy

460

that the current state of knowledge and meteorological forecast does not allow predicting where each individual cloud will form, with which this event could not be predicted in advance.



465

Figure 13. GFS analysis at 18:00 UTC for February 15 2022 for the Petrópolis region. Shades represent surface temperature, isolines represent sea level pressure and the barbs shows wind speed (in knots).

Figure 14 (lower side) shows the radar images of Pico do Couto site, where the formation of the cloud can be seen exactly above the center of the city of Petrópolis. It should be noted that only the residential area of the municipality was affected by the rain, which lasted more than three hours. The accumulated rainfall over the Petrópolis station (Figure 14, upper side) shows the most intense rain between 19:00 and 21:00 UTC. The highest record of 260 mm in just 4 hours, which occurred between the afternoon and evening of February 15th, is unprecedented in the city. It can also be noted the curvature of the storm produced by the southerly winds (represented by blue arrows in the figure), which resulted in its long persistence.

475

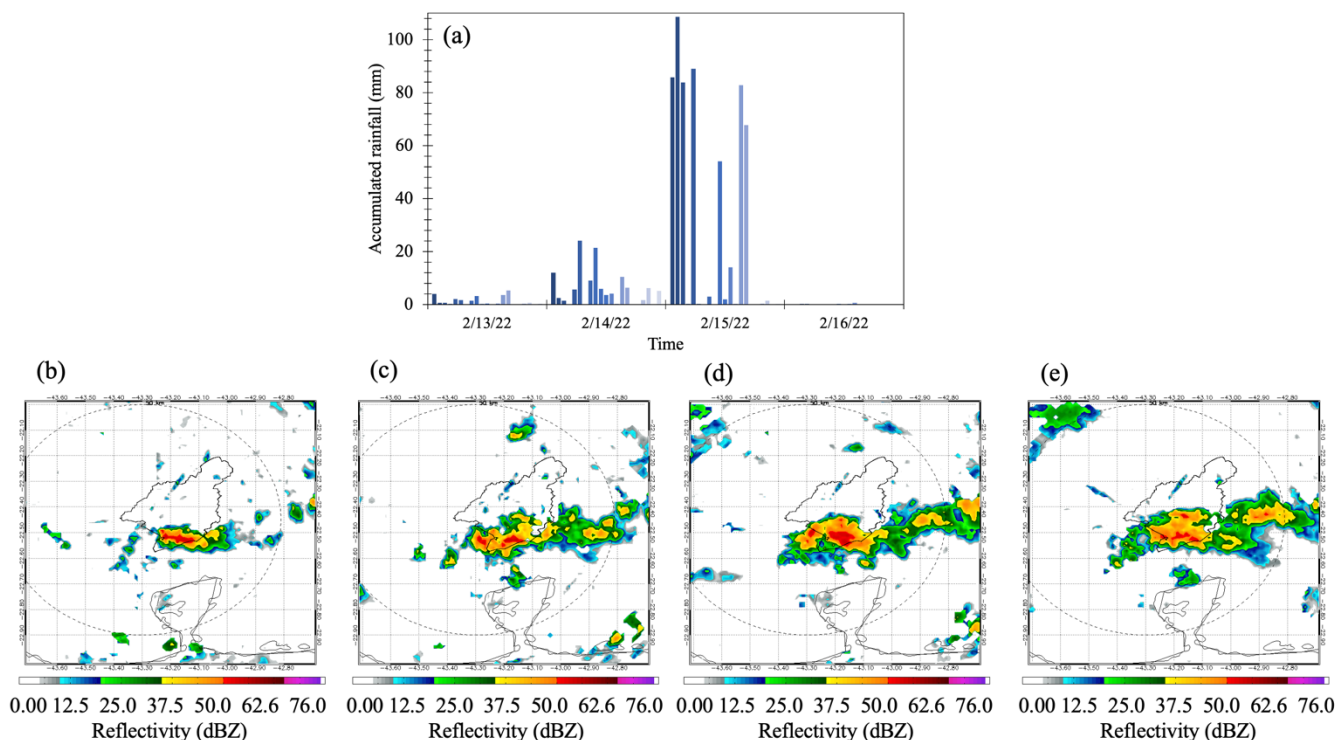


Figure 14. Hourly rainfall for various CEMADEN’s weather station in the city of Petrópolis during February 13-16 2022 (a), radar images at the Pico do Couto site, taken at 7 pm (b), 7:30 pm (c), 8 pm (d) and 8:30 pm UTC for February 15th 2022. (Source: CEMADEN).

480

According to CEMADEN, from a hydrological point of view, the events recorded on February 15, 2022, in the city of Petrópolis were characterized as landslides, flood and flash flood typologies. The municipality’s hydrography indicates the convergence of rivers and streams, which are in an anthropized hydrographic basin while its topographic characteristics resulted in high speed and energy surface runoff. Due to these characteristics and the meteorological event that hit the municipality, there was an increase in the levels of rivers and streams during the intense and concentrated rains. The drainage systems were overloaded and, as a result, the rainwater runs off the surface, causing flash floods and floods.

485

Regarding the occurrence of landslides, the Geotechnical Stations of CEMADEN installed in the municipality of Petrópolis indicate that there was a significant increase in soil moisture during the rainfall event that occurred between 15:30 and 19:00 on February 15, 2022. The monitoring station also indicated that prior to the event, soil moisture was already high since the previous rains exceeded 220 mm/14 days and 350 mm/21 days (recorded in some of the CEMADEN stations). The preceding rise in soil moisture was an inducing, preparatory factor for the occurrence of landslides. The abrupt elevation of soil moisture in a short time interval, due to intense and concentrated precipitation and, consequently, the oversaturation of the ground, provided the triggering of mass movement processes. On the other hand, it was also verified that very high soil moisture was

490

not recorded at deep levels (sensors in depths 2.0 m, 2.5 m and 3.0 m). In other words, a priori, the processes were closely
495 related to intense surface runoff and percolation with very high positive pressure in fractures. The high fracture density favors
the formation of large blocks of rocks on the slopes. Blocks of rocks and colluvial soil deposits were incorporated into the
mass of debris and deposited in valley bottom as a poorly sorted material.

4.2. Tackle urban sprawling for disaster risk management

500 Other than rainfall being the contributing factor, land use change likely worsened the effect of the landslide event. While we
verified an increase in forest cover and urban area and a decrease in agriculture and pasture along the study interval in
Petropolis municipality, the forest located in urbanized region has substantially decreased, as other study showed (Rosi et al.,
2019). Petropolis is in a mountainous region with lower deforestation, compared to less hilly sites (Silva et al., 2020), and
natural regeneration may be happening there (specially replacing old, abandoned pastures), as observed in other parts of the
505 Southeast Atlantic Forest (Silva et al., 2017). In addition, the municipality is part of a protected area (sustainable use: APA
Federal da Região Serrana de Petrópolis), which may help forest conservation and restoration by its management actions.
However, the forest located in places of interest, within the urbanized region, has substantially decreased in extent (Rosi et al.,
2019). At the same time, irregular and unplanned urbanization has been increasing (Guerra, 1995). Thus, public policies, as
the Master Plan, are needed to prevent land use changes that might consequently lead to disasters.

510 In Petrópolis, urbanization has been intensifying since the 1930s, increasing the rural-to-urban migration and unequal urban
development. The population increased rapidly, reaching 75,000 inhabitants in 1940 and 255,000 in 1990. The growth of
tourism and the development of a land market for second homes for citizens from Rio de Janeiro increased the Real Estate
speculation. This speculation excluded low-income households from the formal land market, driving them to occupy hazardous
zones. The rate and form of urbanization expansion overcame precipitation as the most important driver of landslides. Slope
515 areas were unsuitably incorporated into the urban network. In the 1980s, the number of mass movements was larger than those
of the 60s and 70s, in contrast to rainfall values which were lower than the previous decade (Guerra, Gonçalves and Lopes,
2007). Our study revealed that most of the buildings are located in areas of high slope (above 20°), which is not suitable for
human settlements. As such, better management is required to ensure that people inhabit safer areas.

520 Despite not being an official data, the Open Street Maps Platform – OSM - is able to generate geographic information about
human settlements with high quality (Albuquerque et al., 2016). With the need for rapid disaster response, the crowdsourced
data has made it possible to estimate the impact caused by human settlements in areas without cadastral data available.
Examples include the Wenchuan (2008) and Haiti (2010) earthquakes (2008) and Cyclone Idai and Kenneth (2019) in
Mozambique (Li et al., 2020).

525 Dias et al. (2018) created a methodology to associate demographic census data with disaster-prone areas with risk of landslides
and floods, from 1999 to 2012. They found that, out of the total population exposed to risk in Petrópolis, 8.19% were children,
11.24% were elderly, 48.20% male and 51.80% female. In addition, an estimated 26% of at-risk population were living in
subnormal agglomerates (slums), from which 54% had no water supply and 14% had inadequate sanitation services (Dias et

al., 2018). This important information about the conditions of use and occupation of the studied area reinforces the potential contribution of anthropic inducing factors (leaks in pipes, for example) in the deflagration of landslides, and its detailed investigation may even be possible from stability modeling coupled with transient flow analyses (Mendes et al., 2018a; Mendes et al., 2018b). Currently there are no data for 2022 using the same methodology, neither updated data from IBGE – the Brazilian Institute for Geography and Statistics. We retrieved some numbers from the local press and from the municipality’s official communications. Beyond the impacts on human lives and injuries, the economic consequences are also serious, with estimates around R\$ 78,000,000 (FIRJAN, 2022).

Marchezini and Wisner (2017) described a series of dynamic pressures when analyzing disaster risks in Petrópolis: societal deficiencies (lack of planning and investments), business cycles, dense urbanization with population change, deforestation, poor governance, weakening of environmental legislation, real estate speculation and land use change. They also described root causes (social and economic structures, history and culture heritage and ideologies) and factors related to unsafe locations, such as sewage leaking into soil, limited skills and formal education, marginalized groups and individuals, lack of access to formal credit and lack of disaster preparedness.

Disasters cause serious consequences, like deaths, injuries, and economic losses. Preventive actions to tackle risks and disasters may be structural and non-structural. Structural aspects refer to drainage, slopes contention, urban services, and engineering works in general. Non-structural actions refer to environmental education, community meetings and prevention advice, and are as important as the structural ones. Early warnings of disasters are essential to significantly reduce death toll and injuries. For instance, the March 20th event had no more than 4% of the death toll compared to the February 15th event, despite the meteorological drivers of the heavy rainfall in March being of high magnitude. A detailed study is currently underway to go in depth into explaining the difference between the two events and the significance of early warnings in saving lives.

In Petrópolis, there are ongoing preventive works, such as the NUPDEC Vale do Cuiabá: a group of people who live in risk areas and are in contact with the local civil defense to have coordinated actions during a disaster. Complementing the early warnings of disasters, issued by Federal, State and local authorities, Petrópolis also counts on sound warnings (sirens). The National Centre for Monitoring and Early Warnings of Natural Disasters (CEMADEN) is responsible for issuing the warnings, which are forwarded to the Federal civil defense, which distributes the early warnings to State and municipal civil defense agencies. The local civil defense is responsible for evacuating risk areas and addressing rescue activities and shelters establishment. Concerning the civil defense activities, the main needs, according to a recent survey (Brasil, 2021), are related to financial support, structure, and capacity building. Other recurrent theme among the civil defense professionals was the lack of acknowledgement of their work. The actions to improve prevention and response to disasters, therefore, should necessarily consider the improvement of this mentioned deficiencies.

560

5. Conclusion

565 Contrary to what the media reported, the seriousness of the Petrópolis disaster under analysis in the current study was not exclusively due to the large volume of rain. The large death toll had to do with the lack of a precise early warning due to the unpredictable nature of the meteorological event that hit the region, but also to the large number of areas of risk. A set of drivers were responsible for the deadliest disaster in Petrópolis: the heavy rainfall, combined with the already saturated soil, increased unplanned urban sprawl, replacement of vegetation for surfaces with lower capacity of infiltration, and the lack of early warnings, were responsible for the disaster occurred on February 15, 2022.

570 By utilizing available precipitation and human settlement datasets, as well as employing multiple remote sensing data in our analysis, including optical and radar images, we showed that urban sprawling could have a significant effect on slope stability and consequently landslide susceptibility. Several spatial patterns of the February 15, 2022 landslides event were identified. Other than the average rainfall for February 2022 being the heaviest recorded since 1932, the urban part of the city was particularly affected by heavy rainfalls compared to the rural regions. Rainfall evidently influenced soil moisture saturation, although there was higher spatial variability of soil moisture in lower altitudes than in higher altitudes. In our land use assessment, we also recognized that urban sprawling was occurring, accompanying forest losses in urban areas. Together with the mountainous terrain of Petrópolis and the lack of ground deformation detected prior to the landslide, our findings led us to the conclusion that both rainfall, which weakens slopes and washes materials downhill, and human alterations to slopes and surfaces are the main factors contributing to the landslide event.

580 We further emphasize the need for a Master Plan to improve the disaster risk management in Petrópolis. This should include restricting human settlements to within 20° slopes, providing financial support and capacity building for the local civil defense, and limiting land-use changes in landslide-prone regions such as Petrópolis. In the face of climate change, where extreme weather events are expected to become more frequent, it is paramount for Petrópolis to increase its resilience to such disasters. The recent events in 2022 clearly showed that the municipality is still focused on the management of post-impact consequences, instead of actions for disaster risk reduction (DRR). In this sense, efforts should be put to provide a better structure for the civil defense, to integrate the population in prevention planning, to strengthen land use regulations and to improve the risk communication flow.

590 Our focus is only on the February 15, 2022 event. However, in another event on March 20, 2022 the rainfall totals were similarly high and there were a large number of landslides, mudslides and floods. Despite this, the number of deaths was very small. An ongoing study investigates the reasons of such differences. One of the reasons was the meteorological nature of the February 15 event being a mesoscale convective cell that is not predicted (or even predictable) by weather prediction models. Therefore, the CEMADEN warning system did not manage to issue earlier warnings but only when heavy rain started pouring down. On the other hand, the March 20 event was predicted some days before its occurrence, CEMADEN issued precise warnings, the Civil Defense had enough time to remove many residents living in areas of risk and car and bus drivers were

595 informed of the risks and did not take the vehicle to low lying areas under the risk of flooding. It is suggested that the February
15 disaster reduced the number of risky areas for the March 20 event. These are ideas for further discussion.

Data availability

All data produced in this work are available from the corresponding author upon request (enner.alcantara@unesp.br).

600 Author contributions

E. Alcântara and J.A. Marengo developed the study concept. All co-authors contributed to the discussion and the writing process and approved the final version of this text.

Competing interests

The contact author has declared that none of the authors has any competing interests.

605

Acknowledgement

E.A. acknowledge the Brazilian National Council for Scientific and Technological Development (CNPq) for research grants 302575/2021-9. This research was supported by the Singapore Ministry of Education (#Tier2 MOE-T2EP402A20-0001) and the Earth Observatory of Singapore (EOS) via its funding from the National Research Foundation (NRF) of
610 Singapore and the Singapore Ministry of Education (MOE) under the Research Centers of Excellence initiative. JM, APC and RA were funded by the National Institute of Science and Technology for Climate Change Phase 2 under CNPq, grant number 465501/2014-1; Fundação de Amparo à Pesquisa do Estado de São Paulo (FAPESP) grant numbers 2014/50848-9, and the National Coordination for Advanced Education and Training (CAPES), grant number 88887.136402/2017-00.

615 **References**

Albuquerque, J. P. D., Herfort, B. and Eckle, M.: The Tasks of the Crowd: A Typology of Tasks in Geographic Information Crowdsourcing and a Case Study in Humanitarian Mapping, *Remote Sens.*, 8, 1-22, <https://doi.org/10.3390/rs8100859>, 2016.

620 Ansari, H., Zan, FD. and Bamler, R.: Efficient Phase Estimation for Interferogram Stacks, *IEEE Transactions on Geoscience and Remote Sensing*, 56, 4109-4125, 10.1109/TGRS.2018.2826045. 2018.

Ávila, F. F., Alvalá, R.C., Mendes, R.M. *et al.*: The influence of land use/land cover variability and rainfall intensity in triggering landslides: a back-analysis study via physically based models. *Nat Hazards* 105 <https://doi.org/10.1007/s11069-020-04324-x>. 2021.
625

Brasil.: Lei no 12.651, de 25 de maio de 2012.

- 630 Brasil.: Ministério do Desenvolvimento Regional. Secretaria Nacional de Proteção e Defesa Civil Diagnóstico de capacidades e necessidades municipais em proteção e defesa civil [livro eletrônico] : Brasil / coordenação Victor Marchezini. – Brasília, DF : Ministério do Desenvolvimento Regional : Secretaria Nacional de Proteção e Defesa Civil, 2021. PDF. Vários autores. Vários colaboradores. ISBN 78-65-84510-08-1 21-84901 Vários autores. Vários colaboradores. ISBN 978-65-84510-11-1 1. Administração pública – B. 2021.
- 635 Catani, F., Lagomarsino, D., Segoni, S. and Tofani, V.: Landslide susceptibility estimation by random forests technique: sensitivity and scaling issues. *Natural Hazards and Earth System Sciences* 13, 2815-2831, <https://doi.org/10.5194/nhess-13-2815-2013>. 2013.
- 640 Chau, K.T. and Chan JE.: Regional bias of landslide data in generating susceptibility maps using logistic regression: Case of Hong Kong Island. *Landslides*, 2, 280-290, <https://doi.org/10.1007/s10346-005-0024-x>. 2005.
- Chen, C.W and Zebker, H.A.: Two-dimensional phase unwrapping with use of statistical models for cost functions in nonlinear optimization. *Journal of the Optical Society of America A*, 18, 338-351, <https://doi.org/10.1364/JOSAA.18.000338>. 2001.
- 645 Chen ,W., Xie, X., Wang, J., Pradhan, B., Hong, H., Bui, D.T., Duan, Z. and Ma, J.: A comparative study of logistic model tree, random forest, and classification and regression tree models for spatial prediction of landslide susceptibility. *Catena*, 151, 147-160, <https://doi.org/10.1016/j.catena.2016.11.032>. 2017.
- 650 Costanzo, D., Rotigliano, E., Irigaray, C., Jiménez-Perálvarez, J.D. and Chacón, J.: Factors selection in landslide susceptibility modelling on large scale following the gis matrix method: application to the river Beiro basin (Spain). *Natural Hazards and Earth System Sciences*, 12, 327-340, <https://doi.org/10.5194/nhess-12-327-2012>. 2012.
- 655 **CPRM (Geological Survey of Brazil). Avaliação técnica pós-desastre, Petropolis, RJ 2022. www.cprm.gov.br, Ministry of Mines and Energy MME, 9 p. (available from <https://rigeo.cprm.gov.br>). 2022.**
- Dean, W.: A ferro e fogo: a história e a devastação da Mata Atlântica brasileira. Companhia das Letras, São Paulo. 1996.
- 660 Dai, F.C. and Lee, C.F.: Landslide characteristics and slope instability modeling using GIS, Lantau Island, Hong Kong. *Geomorphology*, 42, 213-228, [https://doi.org/10.1016/s0169-555x\(01\)00087-3](https://doi.org/10.1016/s0169-555x(01)00087-3). 2002.
- Dias, H.C., Hölbling, D. and Grohmann, C.H.: Landslide Susceptibility Mapping in Brazil: A Review. *Geosciences*, 11, 1-15, <https://doi.org/10.3390/geosciences111100425>. 2021.
- 665 Dias, M.C.A *et al.*: Estimation of exposed population to landslides and floods risk areas in Brazil, on intra-urban scale. *International Journal of Disaster Risk Reduction*, 31, 449-459, <https://doi.org/10.1016/j.ijdrr.2018.06.002>. 2018.
- 670 Dourado, F., Arraes, T.C. and Silva, M.F.: The “Megadesastre” in the Mountain Region of Rio de Janeiro State – Causes, Mechanisms of Mass Movements and Spatial Allocation of Investments for Reconstruction Post Disaster. *Anuário do Instituto de Geociências*, 35, 43-54, http://dx.doi.org/10.11137/2012_2_43_54. 2012.
- Fattahi H., Agram, P.S., Tymofyeyeva, E. and Bekaert, D.P.: FRInGE; Full-Resolution InSAR time series using Generalized Eigenvectors. American Geophysical Union, Fall Meeting 2019, abstract #G11B-0514. 2019.
- 675 Fonseca, M.J.G., Derze, G.R., Barreto, A.M. and Williams, G.H.: Mapa Geológico do Estado do Rio de Janeiro; Departamento Nacional de Produção Mineral (DPMN): Rio de Janeiro, Brazil, 141p. 1998.

- Fundação SOS Mata Atlântica. Fundação SOS Mata Atlântica. Instituto Nacional de Pesquisas Espaciais. (2018) Atlas dos Remanescentes Florestais da Mata Atlântica período 2016-2017, São Paulo
- 680 García-Rodríguez, M.J., Malpica, J.A., Benito, B. and Díaz, M.: Susceptibility assessment of earthquake-triggered landslides in El Salvador using logistic regression. *Geomorphology*, 95, 172-191, <https://doi.org/10.1016/j.geomorph.2007.06.001>, 2008.
- 685 Gonçalves, L.F.H.: Avaliação e Diagnóstico da Distribuição Espacial e Temporal dos Movimentos de Massa com a Expansão da Área Urbana em Petrópolis-RJ. Ph.D. Thesis, Universidade Federal do Rio de Janeiro-UFRJ, Rio de Janeiro, Brazil. 1998.
- 690 Chen, W., Xie, X., Wang, J., Pradhan, B., Hong, H., Bui, D.T., Duan, Z. and Ma, J.: A comparative study of logistic model tree, random forest, and classification and regression tree models for spatial prediction of landslide susceptibility. *Catena*, 151, 147-160, <https://doi.org/10.1016/j.catena.2016.11.032>, 2017.
- 695 Galarneau, T. J., and L. F. Bosart. Ridge Rollers: Mesoscale disturbances on the periphery of cutoff anticyclones. 21st Conf. on Weather Analysis and Forecasting/17th Conf. on Numerical Weather Prediction, Atlanta, GA, Amer. Meteor. Soc., 3.2, 2006. https://ams.confex.com/ams/WAFNWP34BC/techprogram/paper_94414.htm.
- Goldblatt, R., Jones, N., Mannix, J.: Assessing OpenStreetMap Completeness for Management of Natural Disaster by Means of Remote Sensing: A Case Study of Three Small Island States (Haiti, Dominica and St. Lucia). *Remote Sens* 12, 1-25, <https://doi.org/10.3390/rs12010118>. 2020.
- 700 Guerra, A.: Catastrophic events in Petrópolis city (Rio de Janeiro state), between 1940 and 1990. *GeoJournal* 37, 349-354, <https://doi.org/10.1007/BF00814015>. 1995.
- 705 Guzzetti, F., Carrara, A., Cardinali, M and Reichenbach, P.: Landslide hazard evaluation: A review of current techniques and their application in a multi-scale study, Central Italy. *Geomorphology*. 31, 181-216, [https://doi.org/10.1016/s0169-555x\(99\)00078-1](https://doi.org/10.1016/s0169-555x(99)00078-1). 1999.
- Hersbach, H, Bell, B, Berrisford, P, et al. The ERA5 global reanalysis. *Q J R Meteorol Soc*. 146: 1999– 2049. 2020.
- 710 Huffman, G.J., Bolvin, D.T., Braithwaite, D., Hsu, K.-L., Joyce, R.J., Kidd, C., Nelkin, E.J., Sorooshian, S., Stocker, E.F., Tan, J., Wolff, D.B. and Xie, P. Satellite Precipitation Measurement: Volume 1. Levizzani, V., Kidd, C., Kirschbaum, D.B., Kummerow, C.D., Nakamura, K. and Turk, F.J. (eds), pp. 343-353, 2020.
- 715 IBGE.: Instituto Brasileiro de Geografia e Estatística. Cidades. Available online: <https://cidades.ibge.gov.br/brasil/r28etropolis/panorama> (accessed on 25 September 2018).
- Janowiak, J., Joyce, B., & Xie, P. NCEP/CPC L3 half hourly 4km global (60S - 60N) merged IR V1. 2017. Retrieved from <https://doi.org/10.5067/P4HZB9N27EKU>
- 720 Jolivet, R., Agram, Piyush, S., Lin, Y.N., Simons, M., Doin, M-P., Peltzer, G and Li, Z.: Improving InSAR geodesy using Global Atmospheric Models. *Journal of Geophysical Research: Solid Earth* 119, 2324-2341, <https://doi.org/10.1002/2013JB010588>, 2014.
- 725 Kanwal, S., Atif, S. and Shafiq, M.: GIS based landslide susceptibility mapping of northern areas of Pakistan, a case study of Shigar and Shyok Basins. *Geomat. Nat. Hazards Risk* 8, 348-366, <https://doi.org/10.1080/19475705.2016.1220023>, 2017.

- Komac, M. and Ribičič, M.: Landslide susceptibility map of Slovenia at scale 1:250,000. *Geologija*, 49, 295-309, <https://doi.org/10.5474/geologija.2006.022.2006>.
- 730 Li, H., Herfort, B., Huang, W., Zia, M and Zipf, A.: Exploration of OpenStreetMap missing built-up areas using twitter hierarchical clustering and deep learning in Mozambique, *ISPRS Journal of Photogrammetry and Remote Sensing*, 166, 41-51, <https://doi.org/10.1016/j.isprs.2020.05.007>. 2020.
- 735 Lin, Y. N., Park, E., Wang, Y., Quek, Y.P., Lim, J., Alcântara, E. and Loc, H. H.: The 2020 Hpakant Jade Mine Disaster, Myanmar: A multi-sensor investigation for slope failure. *ISPRS Journal of Photogrammetry and Remote Sensing*, 177, 291-305, <https://doi.org/10.1016/j.isprs.2021.05.015>. 2021.
- Maddox, R. A., L. R. Hoxit, C. F. Chappell, and F. Caracena. Comparison of meteorological aspects of the Big Thompson and Rapid City flash floods. *Mon. Wea. Rev.*, 106, 375–389, 1978.
- 740 Marengo, J.A., Alves, L.M. The 2011 intense rainfall and floods in Rio de Janeiro. *Bulletin of the American Meteorological Society*, v. 93, p. S176, 2012.
- Marchezini, V., Wisner, B.: Challenges for vulnerability reduction in Brazil: Insights from the PAR framework. In *Reduction of vulnerability to disasters: From knowledge to action*. Edited by Marchzini V, Wisner B, Londe L. 2017.
- 745 Mendes RM, Andrade MRM, Graminha CA *et al.*: Stability Analysis on Urban Slopes: Case Study of an Anthropogenic-Induced Landslide in São José dos Campos, Brazil. *Geotech Geol Eng* 36, 599-610, <https://doi.org/10.1007/s10706-017-0303-z>. 2018a.
- 750 Mendes, R.M., Andrade, M.R.M., Tomasella, J., Moraes, M.A.E. and Scofield, G.B.: Understanding shallow landslides in Campos do Jordão municipality – Brazil: disentangling the anthropic effects from natural causes in the disaster of 2000, *Nat. Hazards Earth Syst. Sci.*, 18, 15-30, <https://doi.org/10.5194/nhess-18-15-2018>, 2018b.
- 755 Minghini, M. and Frassinelli, F.: OpenStreetMap history for intrinsic quality assessment: Is OSM up-to-date?. *Open geospatial data softw. stand.* 4, 1-17, <https://doi.org/10.1186/s40965-019-0067-x>. 2019.
- Mitchell, M. J., R. W. Arritt, and K. Labas, 1995: A climatology of the warm season Great Plains low-level jet using wind profiler observations. *Wea. Forecasting*, 10, 576–591, [https://doi.org/10.1175/1520-0434\(1995\)010<0576:ACOTWS>2.0.CO;2](https://doi.org/10.1175/1520-0434(1995)010<0576:ACOTWS>2.0.CO;2).
- 760 Montgomery, D.R., Schmidt, K.M., Greenberg, H.M. and Dietrich, W.E.: Forest clearing and regional landsliding. *Geology* 28, 311-414, [https://doi.org/10.1130/0091-7613\(2000\)28%3C311:FCARL%3E2.0.CO;2](https://doi.org/10.1130/0091-7613(2000)28%3C311:FCARL%3E2.0.CO;2). 2000.
- 765 Myers, N., Mittermeier, R.A., Mittermeier, C.G., Fonseca, G.A.B. and Kent, J.: Biodiversity hotspots for conservation priorities. *Nature* 403, 853-858, <https://doi.org/10.1038/35002501>. 2000.
- Nehren, U. *et al.*: (eds.) *Strategies and Tools for a Sustainable Rural Rio de Janeiro*, Springer Series on Environmental Management, https://doi.org/10.1007/978-3-319-89644-1_20. 2018.
- 770 Ohlmacher, G.C. Plan curvature and landslide probability in regions dominated by Earth flows and Earth Slides. *Engineering Geology* 91, 117-134, <https://doi.org/10.1016/j.enggeo.2007.01.005>. 2007.
- 775 Penha, M.M., Ferrari, A.L., Junho, M.C.B., Souza, S.L.A. and Brennes, T.L.: *Projeto Carta Geológica do Estado do Rio de Janeiro: Folha Itaipava; v. 1; Convênio DRM/IG-UFRJ: Rio de Janeiro, Brazil*. 1981.

- Reichenbach, P., Rossi M., Malamud, B., Mihir, M. and Guzzetti, F.: A review of statistically-based landslide susceptibility models. *Earth-Science Reviews*, 180, 60-91, doi:10.1016/j.earscirev.2018.03.001. 2018.
- 780 Reis, A.A., Fernandes, W.S., Ramos, M-H. Assessing two precipitation data sources at basins of special interest to hydropower production in Brazil. *Brazilian Journal of Water Resources*. 25, 2020.
- 785 Rosi, A., Canavesi, V., Segoni, S., Nery, T.D., Catani, F. and Casagli N.: Landslides in the Mountain Region of Rio de Janeiro: A Proposal for the Semi-Automated Definition of Multiple Rainfall Thresholds, *Geosciences*, 9, 1-15, doi:10.3390/geosciences9050203. 2019.
- Schlossmacher, E.J.: An Iterative Technique for Absolute Deviations Curve Fitting. *Journal of the American Statistical Association*. 68:344 <https://doi.org/10.2307/2284512>. 1973.
- 790 Silva, R.F.B., Batistella, M., Moran, E.F. and Liu, D.: Land changes fostering Atlantic Forest transition in Brazil: Evidence from the Paraíba Valley. *The Professional Geographer*. 69, 80-93, <https://doi.org/10.1080/00330124.2016.1178151>. 2017.
- Souza, C.M.Jr. *et al.*: Reconstructing Three Decades of Land Use and Land Cover Changes in Brazilian Biomes with Landsat Archive and Earth Engine. *Remote Sens* 12, 1-17, <https://doi.org/10.3390/rs12172735>. 2020.
- 795 Srivastava, P.K., Mehta, A., Gupta, M., Singh, S.K. and Islam, T.: Assessing impact of climate change on Mundra mangrove forest ecosystem, Gulf of Kutch, western coast of India: a synergistic evaluation using remote sensing. *Theoretical and Applied Climatology* 120, 685-700, <https://doi.org/10.1007/s00704-014-1206-z>. 2015.
- 800 Wang, J., Dong, X., Kennedy, A., Hagenhoff, B., Xi, B. A regime-based evaluation of southern and northern great plains warm-season precipitation events in WRF. *Weather Forecasting*, 34, 805– 831, 2019.
- Younes-Ibrahim, S., Pinheiro, M.A. and Pardo, C.R. Testemunhos de Sobreviventes ao Desastre de 2011 em Petrópolis: Abordagem Psicossocial em um Campo Ferido. *Estud. pesqui. Psicol* 19, 366-386, <https://doi.org/10.12957/epp.2019.44279>. 2019.